26th International Congress of Mechanical Engineering
November 22-26, 2021, Virtual Congress, Brazil

COBEM-2021-0410
DESIGN OF A HIGH PEFORMANCE ENGINE FOR AMATEUR MOTORSPORTS

Matheus Strapasson
Mario Martins
Eduardo Antocheviez Flores
Igor Rodrigues dos Santos
Federal University of Santa Maria
strapa.matheus@gmail.com
mario@mecanica.ufsm.br
eduardo.an.flores@gmail.com
igor.santos@mecanica.ufsm.br

Abstract. *This paper presents the development of a high performance internal combustion engine for motorsports applications. The base for this project was an inline four-cylinder sport bike engine which is compact, lightweight and has parts that ease a new configuration. The chosen architecture for this new engine was a 90 degrees V8 that offers more power density than the original configuration and allows the usage of a great portion of the original engine parts. Changes in the engine block and crankshaft were made as well as to the engine mounts. These modifications and the design of the engine were made with the CAD software SolidWorks. With the aid of the CAE software GT-Power,1-D thermodynamic simulations were performed. The engine got up to 217 kW at 11,000 rpm. With the same software, the magnitude and direction of the forces in the engine block and main bearings were obtained.*

Keywords: *racing engines, crankshaft, engine block, engine simulation.*

1. INTRODUCTION

Since the internal combustion engine was invented, a constant development of performance and efficiency was required. In this development process, a very high contribution was given from motorsports which adopted the internal combustion engine as the best suitable power unit for racing. (Chiodi et al. 2011). Besides, of all high-performance engineering industries, motorsport perhaps best exemplifies the unique combination of key engineering and business elements vital for swift, industry-focused, successful, high-technology product advancement (Meechan 2006).

Taking the environmental aspects into account, whose impact of automotive industry is growing, attempts were made to introduce new F1 engines of design closer to those used in general automotive sector (STĘPIEŃ 2016). Since 1995, in F1 racing championships, a V-type engine was imposed by the championship rules (McLaren 2016). This can be explained by the fact that V-type engines have gradually pushed out any other engine type because they are compact and can be constructed very rigidly without requiring further strengthening to the chassis to ensure stiffness (Boretti 2013). Also, over the years, these rules demanded an engine downsizing and an improve of fuel efficiency, leading the manufacturers to push their engineers to design and develop a fuel-efficient engine for optimum power delivery and increased reliability (Bopaiah and Samuel 2020)

For high performance vehicles, flat-plane crankshafts are more desirable than cross-plane crankshafts due its lower inertia moment, which allows reduce system mass and higher engine speeds thus increasing power-weight ratio (Costa 2020). Besides, the blowdown interference that occurs in cross-plane and flat-plane crankshaft architectures is worse in the former which impacts negatively in-cylinder scavenging process (Corvaglia, Böger, and Bevilacqua 2019).

Therefore, considering all these factors, this paper aims to develop a concept for a high-performance engine focusing on the adaptation of an engine that already exist on the market. The engine developed must be powerful, reliable, easy to manufacture and fit under the hood of a racing car. This brings challenges such as packaging and the need for the engine to adapt to this car's components. The present work will go through the choice of which engine was used, critical design features and simulations to evaluate the brake power of the engine and the forces acting on its main bearings.

2. ENGINE DESIGN AND CHARACTERISTICS

The criterion for choosing which engine to be used as a starting point for the design of the new engine is, of the engines available in the market, the one with the most adaptability. This means that engine parts must make the adaptation to other engine layouts easier and with least changes to engine components as possible. Using original parts of the engine, not only simplifies fabrication, but also reduces the overall cost of the engine and lessens the time it takes to develop the engine.

Therefore, the chosen engine was a sport motorcycle engine. This choice was made by the fact that this engine has its cylinder block separated from the crankcase, making the adaptation to other arrangements much easier than other engines. Figure 1 shows the cylinder block and Table 1 shows the engine characteristics.

Figure 1. Cylinder block.

Table 1 – Engine characteristics.

Engine characteristics	
Engine type	4-stroke, DOHC, liquid-cooled
Displaced volume	1.299 L
Compression ratio	11:1
Bore x Stroke	81 mm x 63 mm
Maximum brake power	129 kW @ 9500 rpm
Maximum brake torque	134.23 Nm @ 7000 rpm
Firing order	1-2-4-3
Distance between cylinder centers	88 mm
Dimensions (LxWxH)	520 mm x 540 mm x 620 mm

2.1 Cylinder arrangement

Since this engine has 4 cylinders in line, there are three arrangements that can be chosen to preserve the most original parts as possible: 4 cylinders in line, 8 cylinders in line or 8 cylinders in "V". Since 8 cylinders in line makes the engine and the crankshaft lengthy and heavy, this configuration was disregarded. Between 4 cylinders in line and 8 cylinders in "V", the "V" configuration was chosen because it is compact and can be constructed very rigidly without requiring further strengthening to the chassis to ensure stiffness (Boretti 2013) and it also has more power density than the inline configuration. Besides, the first basic method for giving performance or sporty impression to the customer is loudness. Surveys have shown that loudness has a distinct effect in the performance impression, with louder sounds giving a higher performance impression (Hiscutt and Ishikawa 2008) and the sound of V8 engines has its own cultural appeal that cannot be replaced by the modern four-cylinder naturally aspirated or turbocharged engines (Luján et al. 2010).

Choosing the "V" arrangement allows the usage of various parts such as cylinder blocks, connecting rods, pistons, cylinder head and valvetrain. In this sense, there was the need to place two-cylinder blocks side by side in crankcase with its timing chains at opposite sides of crankcase. Another reason for this placement is that the intake and water gallery connections of both cylinder blocks remains on the same side resulting in simpler connections. As they are facing away from each other, the camshafts of the first cylinder head will be rotating in different directions from the ones in the second since the original engine has a clockwise rotation. To solve this, a gear was made in the crankshaft that connects with an additional gear to change the rotation direction of camshafts. In the same axle of this additional gear was placed a second gear to drive the camshafts, spinning in clockwise rotation. Since the distance between the drive gear and the camshafts was changed, the stock chain cannot be used in this cylinder head.

As said before, in the original engine, the camshafts are driven by the crankshaft with a chain and to preserve the lubrication of this component, the engine has covers bolted in the crankcase that make a chamber for the chain and thus the oil that lubricates the gears in the camshafts also lubricates the chain, as then falls off to the sump by an opening in the crankcase. In the V8 engine this is similar, covers bolted to the crankcase were also used, the difference is that V8 has two-cylinder heads and therefore, two sides to cover. So, there was the need to make two covers instead of one, adding length and complexity to the engine.

2.2 Crankshaft design and configuration

(Hoag and Dondlinger 2016) said that there are two possibilities for crankshaft configuration in a V8: a flat-plane crankshaft or a cross-plane crankshaft (cruciform crankshaft). The former is similar in appearance to that of a four-cylinder engine but with two connecting rods sharing each throw, the latter has its crankpins 90º apart from each other, creating two planes that cross one another. The cross-plane crankshaft runs more smoothly than a flat-plane crank, since the last produces free second order forces that cannot be balanced with use of counterweights, only with balance shafts, therefore the planar crank train would generate higher loading and forces into the engine structure at the middle main bearing (McLuckie and Barrett 2005). It is worth mentioning that primary and secondary forces increase with engine speed and with unbalanced masses and do not change with engine operating conditions. Turning back, the cross-plane crankshaft presents free centrifugal and first order forces that can be balanced by counterweights (Corvaglia, Böger, and Bevilacqua 2019). However, in cross-plane crankshafts, two cylinders per bank always fire in direct succession, this means that the exhaust pressure pulse of the subsequent cylinder already occurs while the exhaust valves of the previously ignited cylinder are still open. As a result, exhaust is pushed back into these cylinders causing inefficient gas exchanges and therefore, decreasing performance. Also, the residual gases promote knocking which limits the engine potential (Penzel, Belivacqua, and Raab 2017).

Figure 2 shows the interference of the exhaust pulses in a 90º V8 with cross-plane crankshaft. When the exhaust valves of cylinder 3 open, the outflowing burnt gas causes a strong increase on pressure in the exhaust manifold and in the ports of all cylinders on the same bank. The pressure at the exhaust port of cylinder 1 stays high even during the overlap of the opening of its intake and exhaust valves, degrading the scavenging process. In flat-plane crankshaft this effect is lessened because in the same cylinder bank, exhaust blowdowns are evenly spaced in 180º each, similarly to engines with 4 cylinders in line (Corvaglia, Böger, and Bevilacqua 2019).

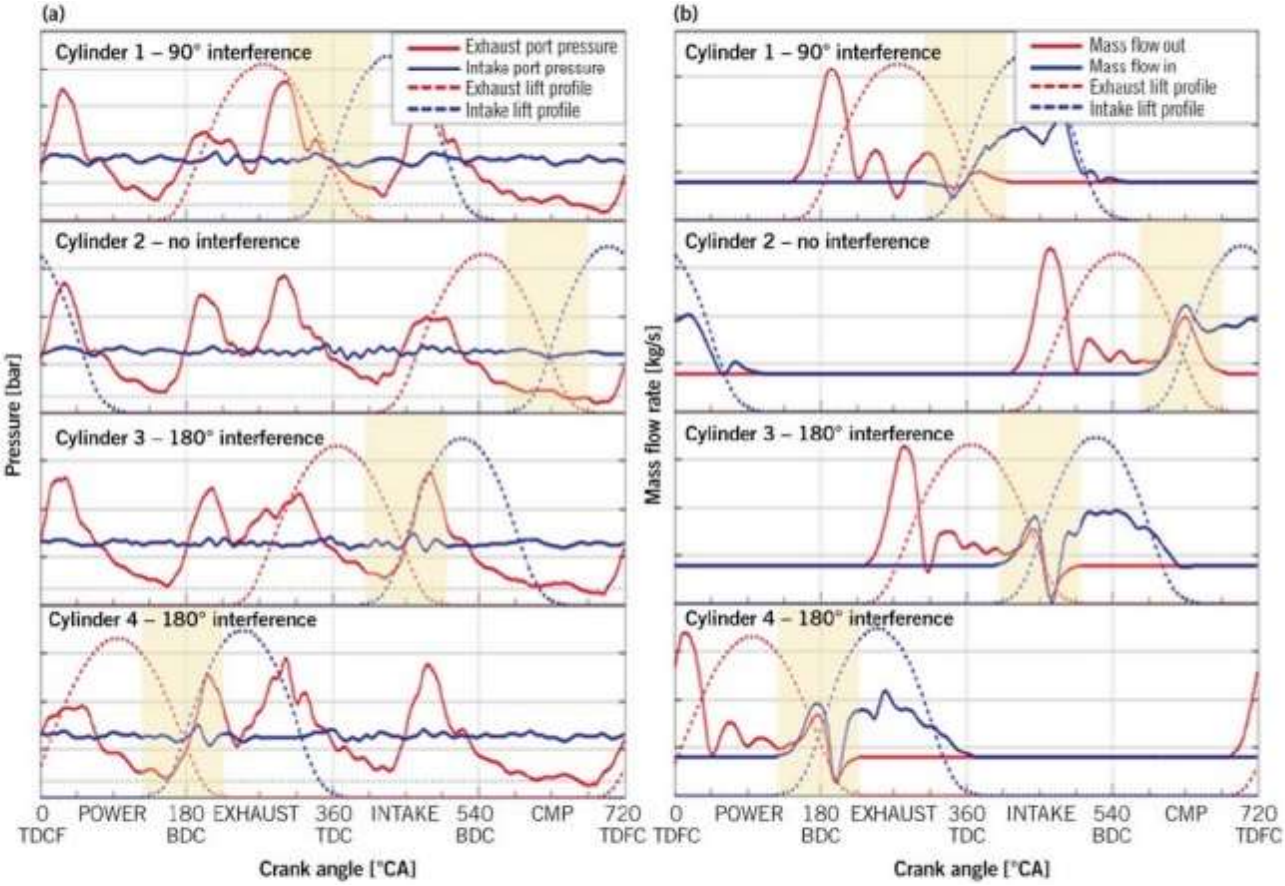

Figure 2. (a) Pressure at the intake and exhaust ports; (b) mass flow rate through the exhaust and intake valves of the cylinders on the same bank of a cross-plane V8 engine at 2200 rpm and full load (Corvaglia, Böger, and Bevilacqua 2019).

The cross-plane crankshaft also has more mass and bulkier counterweights. Hence, it has a higher moment of inertia than the flat-plane crankshaft. This means that flat-plane crankshaft is more responsive, leading to rapid acceleration and achieving higher engine speeds as possible. Taking that into account, the chosen crankshaft configuration for this engine was the flat-plane crankshaft since for high performance applications, smoothness and refinement are not as important as power.

The design of the crankshaft was made in a way that the connecting rods of the original engine could be used. The length of the crankpin was 22 mm and the width of the connecting rod was 21 mm. In that high performance engine, the crankpin diameter was preserved, but a length of one crankpin was added for two connecting rods be able to share the same throw, at the expense of reduce counterweight width. The distance between the connecting rods of the same bank should be equal to the distance between cylinder centers to assure alignment.

To transport the oil from the main bearings to the connecting rod bearings, drillings across the crankshaft were made. These drillings were made in a way so that the rotation of the engine would assist the feeding of oil to the bearings. (Hoag and Dondlinger 2016) said that the breakout of the oil hole in the crankpin should not be located between 0 and 45º after TDC, because the high rod loadings increase the oil pressure above the system pressure and prevents feeding. Alternatively, (Manning 2012) recommends breakout between 30º and 60º ahead of TDC, because the rotation of the crankshaft assists oil feeding in the crankpin. Knowing this, the breakout angle of 55º was chosen. (Manning 2012) also gives typical values for the diameter of the oil hole in the crankshaft, this range lies between 5 and 8 mm. To minimize the material removal and, consequently, less stiffness in the crankshaft, the diameter of 5 mm was chosen.

2.3 Vee angle and firing order

(Manning 2012) says that for a good engine refinement and lower NVH (Noise, Vibration, and Harshness), even firing intervals should be used. Also, (Hoag and Dondlinger 2016) stated that if an even spacing between the gas pressure forces is to be achieved, the product of the total number of cylinders and the "V" angle must be equal to 360º or 720º. With this, if 8 cylinders are to be used, then a 90º crank angle or a 45º crank angle between firing pulses is needed. Another common angles used in a V engine are 60°, 72° and 75°, but since those angles will give this engine uneven firing pulses and thus poorer NVH, they were not used. It must be noted that, in a V8 with a flat-plane crankshaft, the angle between the cylinder banks is the equal to the interval of the firing pulses from one bank to another. (Heisler 2002) claims that in a 90º V8 flat plane crankshaft, the secondary forces vertical components in each four-cylinder bank are cancelled out due to the 90º inclination, but these secondary forces combine in a horizontal component and produce a secondary force disturbance equal to 1.414 times the total secondary force on one bank of cylinders. This means that there will be an inherent horizontal unbalance in this engine. Then, with a 45º interval, this angle makes the assembly of the two-cylinder banks impossible, so a 90º angle was used. That said, the sequence of the firing order of the original engine was preserved. Figure 3 shows the firing order.

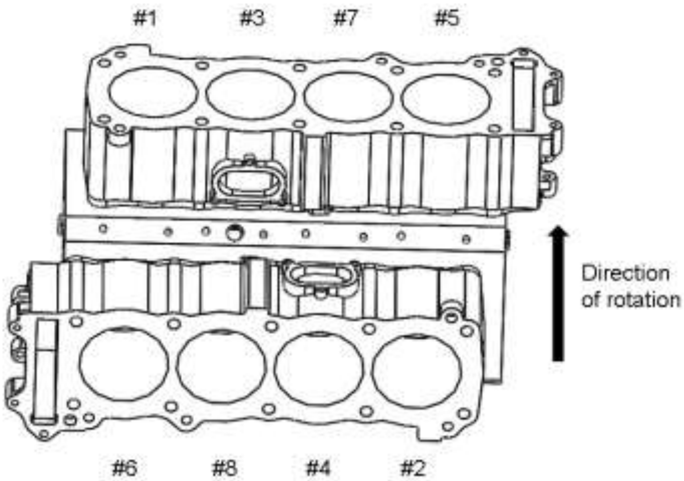

Figure 3. Firing order.

2.4 Brake power

In Eq. (1) it can be concluded that the displaced volume and the angular velocity of the engine are directly proportional to the brake power (Heywood 2018).

$$P = bmep * V_d * N/n_R, \quad (1)$$

where P, $bmep$, V_d, N and n_R are brake power, brake mean effective pressure, displaced volume, engine speed and number of crank revolutions for each power stroke, respectively."

By doubling the displaced volume by adding another cylinder bank, it can be expected that brake power is also doubled, however, by adding more cylinders several losses like friction, heat and pumping losses increase together with power lessening the value of the brake mean effective pressure, hence, reducing the brake power. Thus, is expected that the brake power increase less than twice the brake power of original engine. To estimate this value correctly, the engine was simulated in the Computer Aided Engineering (CAE) software GT-Power.

2.5 Crankcase

The original engine crankcase was split into an upper crankcase and a lower crankcase which upper crankcase makes the mating with the cylinder block while lower crankcase mates with the sump. They are held together by bolts.

A critical block layout dimension for the upper crankcase is the deck height. This is the distance from the crankshaft main bearing centerline to where the cylinder head mates to the block. The deck height is determined by the following equation (Hoag and Dondlinger 2016):

$$Minimum\ Deck\ Height = 0.5 \cdot Stroke + Conneting\ Rod\ Length + Piston\ Crown\ Height, \quad (2)$$

where the connecting rod length is the distance between bearing centerline and piston pin centerline and the piston crown height is the distance between its pin centerline and the top of the crown."

Since the cylinder block is separated from the crankcase and the deck height is the sum of the distance between the main bearing center to the bottom of cylinder block with cylinder block height, Equation (2) can be adapted to calculate the distance between the center of the main bearing to the face where the cylinder block mates the crankcase. The following equation makes this relation:

$$Main\ Bearing\ to\ Cylinder = 0.5 \cdot Stroke + Connecting\ Rod\ Length + Piston\ Crown\ Height - Cylinder\ Block\ Height, \quad (3)$$

Measures taken for the values connecting rod length and the piston crown height revealed that the former have 119.5 mm and the latter 25 mm. The cylinder block height was also measured showing a value of 88 mm. With this, the solution of Equation (3) gives a value of 88 mm. For safety purposes, a value of 89 mm was chosen for the manufacturing of the first prototype, making adaptations as necessary.

The lower part of the crankcase was made a bedplate because this structure provides the best overall stiffness to the engine and are also cost effective (Manning 2012), this is especially good in blocks made of aluminum where stiffness is a critical design factor. On the other side, bedplates make the crankcase difficult to seal, since it requires the use of liquid sealant as the use of a gasket would impact bearing clearance (Hoag and Dondlinger 2016). To help with this issue, additional bolts were placed in the perimeter of the crankcase, to assist sealing with clamping force.

(Manning 2012) states that the bedplate is also good for withstanding the transverse loads generated in V shaped engines because of the high stiffness and high number of attached bolts. Figure 4 shows the designed crankcase.

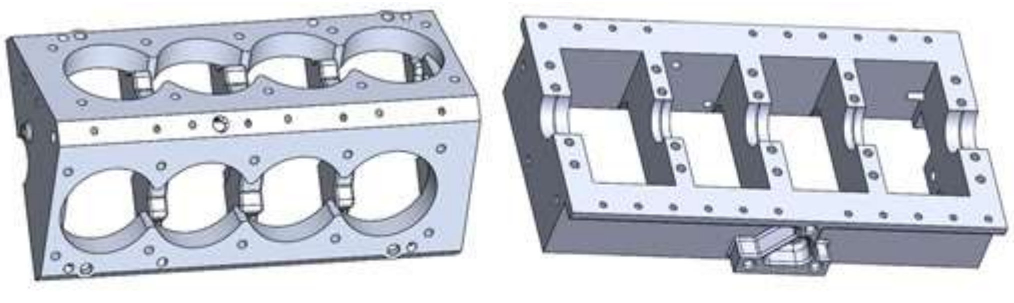

Figure 4. Adapted upper crankcase and bedplate.

2.6 Water and oil galleries

The water gallery is another reason why this motorcycle engine was chosen since it does not pass through the crankcase. In this engine, the water enters in cylinder block and passes through built-in galleries on cylinder block and on cylinder head and then goes to radiator. This dismisses the need to make a water gallery in the new engine, simplifying the fabrication significantly.

In the original engine the main oil gallery was below the crankcase and in the new engine, like most V8 engines, the main oil gallery is located above the main bearings and between the cylinder banks.

2.7 Oil Sump

In a race, where high accelerations act on the engine, there is a risk of oil starvation at high engine speeds, because the oil spends more time inside the crankcase than in the oil pan, reducing the oil level in the sump (Osman 2012).

This starvation of oil damages the engine and reduces its reliability and its lifespan. Furthermore, the dry sump was chosen for packaging reasons and because the engine can be mounted lower than with a wet sump, this also lowers the center of gravity of engine, improving the handling of the car. (Khanna et al. 2019) achieved a decrease in the center of gravity of a Formula SAE engine of 26.5 mm by placing a dry sump system instead of a wet sump.

3. RESULTS AND DISCUSSIONS

That said, the design of the engine was made with CAD. The engine was then assembled to verify and correct possible interferences that were present in the model. Figure 5 shows the complete assembly of the engine ready to be mounted in a car and the V8 crankshaft. This figure depicts the significant extension of the crankshaft to support the flywheel, adding concerns about the effects of torsion and bending in the crankshaft. These effects should be analyzed with a finite element analysis to validate the design. In comparison to original crankshaft, this one has an additional length of 140 mm.

(a)

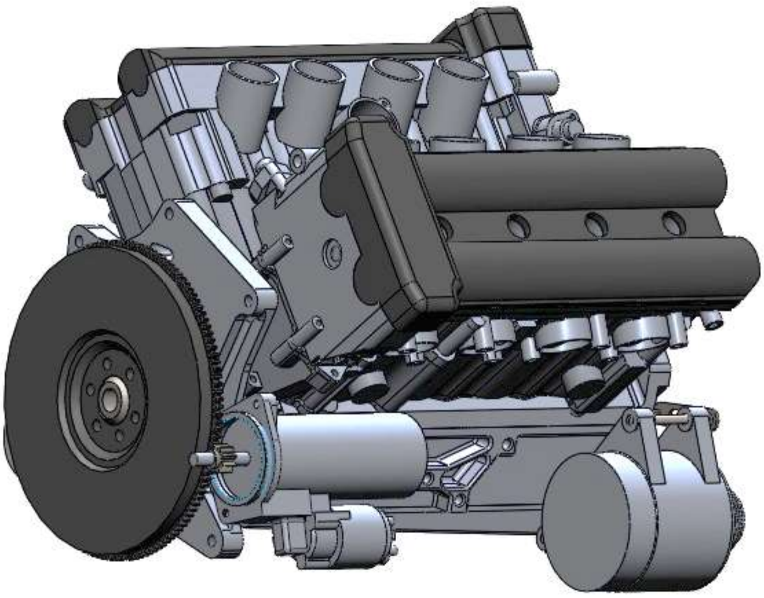

(b)

Figure 5. (a) Engine assembly in CAD and (b) V8 crankshaft.

The narrow difference in width of V8 engine to original inline 4-cylinder is because the latter possesses a built-in structure for the gearbox in the crankcase, adding to the width of the original engine significantly. Alternatively, the reduction in height experienced in the V8 is due to the angle of the cylinder banks and the use of the dry sump. The substantial increase in length derived mostly from the adaptation to mount the engine in a car, however, the cylinder offset and the addition of one cover also had a considerable influence. Table 2 summarizes the characteristics of the designed V8 engine.

Table 2 – V8 engine characteristics.

Engine type	4-stroke, DOHC, liquid-cooled
Displaced volume	2.6 L
Dimensions (LxWxH)	625 mm x 568 mm x 444 mm

Using the geometric data obtained in the design, a 1-D thermodynamic simulation was made on GT-Power software to analyze the engine performance and structural loads. The engine was simulated for both flat and-cross-plane crankshafts to evaluate which architecture gives highest performance. Figure 7 presents the engine power obtained in the engine simulation for each crankshaft architecture.

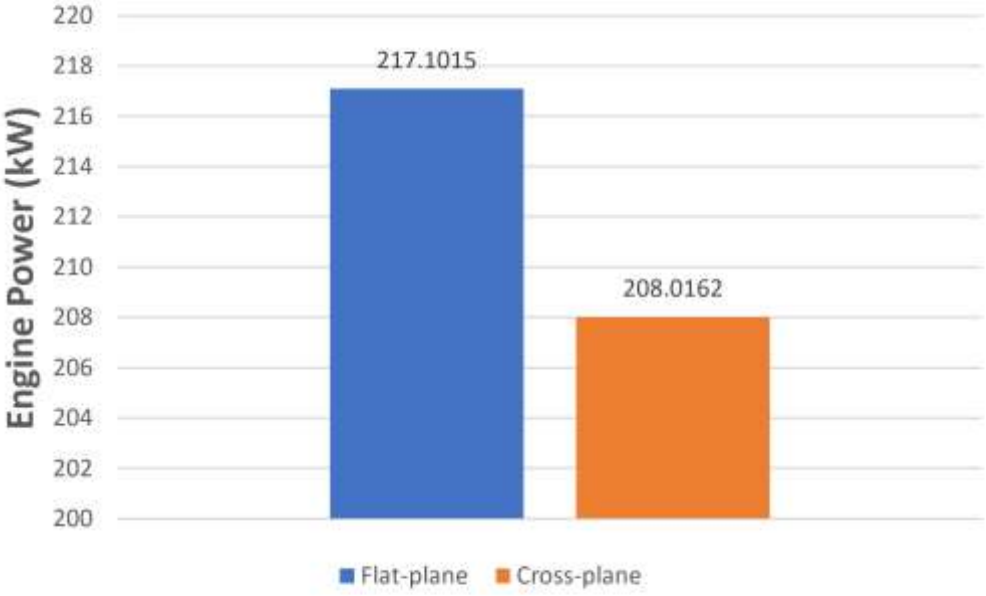

Figure 7. Comparison between engine power for simulated engine with flat-plane crankshaft and cross-plane crankshaft at maximum power (11,000 rpm).

As can be seen, the flat-plane crankshaft had 9.1 kW more power than cross-plane crankshaft. As expected, this difference is due to higher blowdown interference in cross-plane crankshafts, as stated by (Corvaglia, Böger, and Bevilacqua 2019). Figure 8 shows the blowdown interference influence on volumetric efficiency at maximum power.

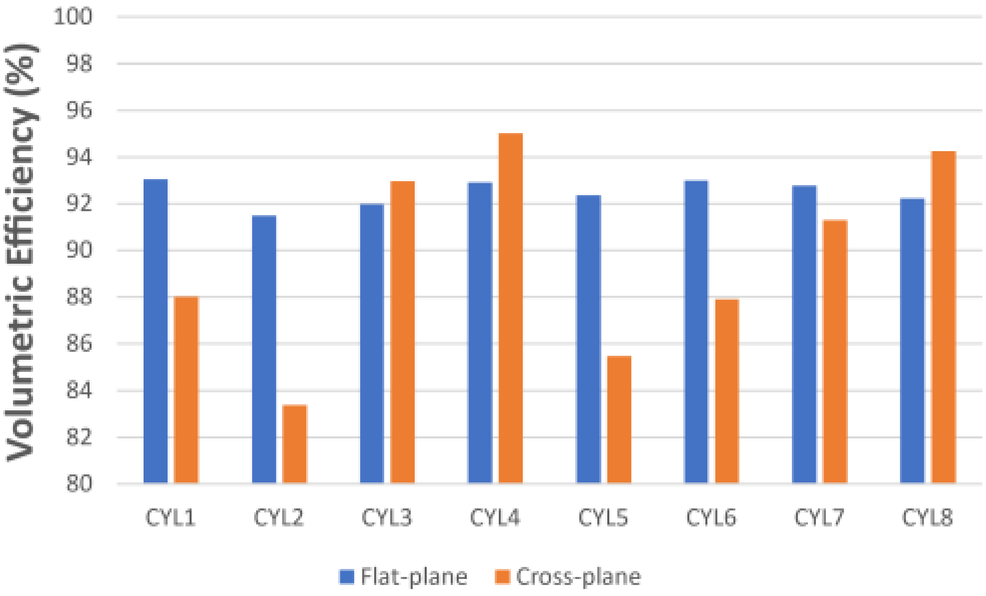

Figure 7. Blowdown interference influence on volumetric efficiency at maximum power (11,000 rpm).

The volumetric efficiency is significantly reduced with cross-plane architecture, lessening the engine power. Therefore, for better engine power, the flat-plane crankshaft is more recommended. Figure 6 depicts the engine brake power curve obtained.

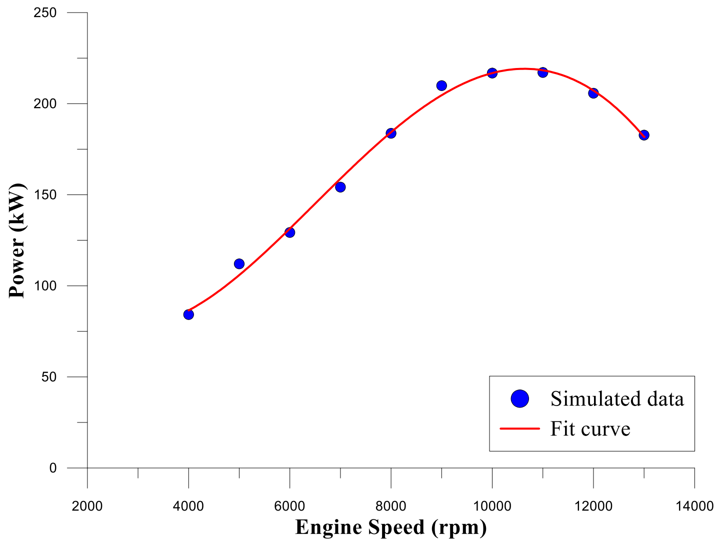

Figure 6. Simulated brake power curve.

The results show a maximum value of brake power near of 217 kW at 11,000 rpm, less than twice original engine brake power as expected with regards to the theory presented in section 2.4.

For safety purposes, the acting forces on the bearings were analyzed at 12,000 rpm because of the loads acting on the main bearings promoted by inertial forces are higher than at 11,000 rpm. Figure 8 depicts the forces acting on the engine and on each bearing along the crank angle with its horizontal and vertical components. In these forces there are 3 critical points for the structural integrity of the engine: at crank angle when the vertical forces are stronger, at the crank angle when the horizontal forces are stronger and at crank angle which the combined vertical and horizontal components are stronger. The results show that the vertical component of the forces was more critical than the horizontal components mainly on the middle bearing (see Table 3). This behavior is due to incorrect use of counterweights to balance the engine, since the same counterweights of original 4 cylinder engine were used. Therefore, is required a further analysis of several counterweight masses and geometries to set an optimum design to balance the engine.

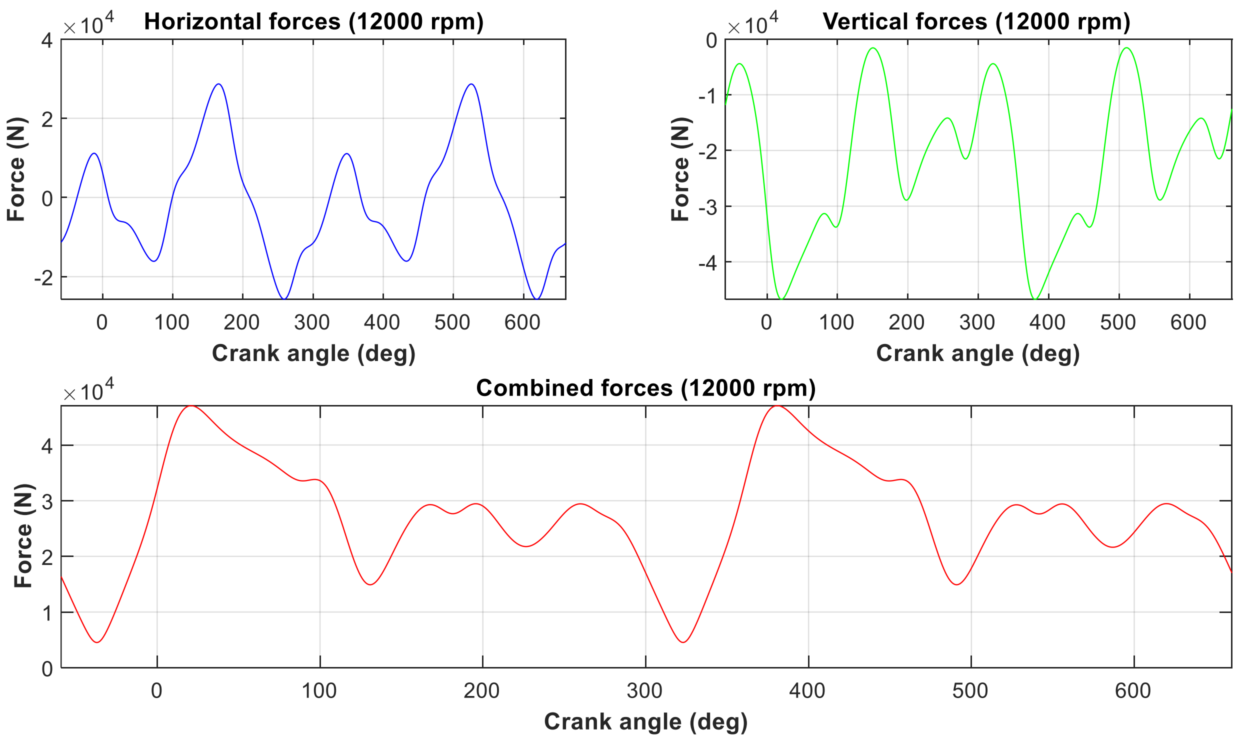

Figure 8. Forces acting on the engine block.

Table 3 – Forces acting on the engine main bearings. The bearings are numbered from 1 to 5 starting from the front of the engine.

	Maximum horizontal forces		**Maximum vertical forces**		**Maximum combined forces**	
Crank angle of event	**166° After TDC firing**		**381° After TDC firing**		**382° After TDC firing**	
Bearings	**Magnitude (kN)**	**Angle of incidence (º)**	**Magnitude (kN)**	**Angle of incidence (º)**	**Magnitude (kN)**	**Angle of incidence (º)**
Bearing #1	16	213,7	17,67	58,7	17,53	60
Bearing #2	7,01	353,6	13,31	309,3	13,46	309,1
Bearing #3	34,95	21,4	37,76	253,2	37,92	253,9
Bearing #4	14,5	4,3	22,53	239,7	22,43	239,5
Bearing #5	15,5	218	4,18	103,4	4,48	104,1

4. CONCLUSION

The present work addressed some important design features when adapting an engine to racing applications. It was concluded that a flat-plane crankshaft is the better choice when designing the engine to high performance applications because it is more responsive and lighter as the cross-plane crankshaft. Not only that, but the flat-plane crankshaft does not have the same problem with gas exchanging as does the cross-plane crankshaft.

Through the geometrical data of designed engine, the engine was modeled and simulated on GT-Power CAE software. The simulation results demonstrated a volumetric efficiency reduction due to higher blowdown interference with cross-plane crankshaft architecture in comparison with flat-plane crankshaft. This reduction lessens the engine power output, therefore, making flat-plane crankshafts more attractive to high performance engines. The engine power curve achieved a preliminary figure of 217 kW at 11,000 rpm.

In the analysis of the forces acting in the main bearings, the inherent unbalance of the second order forces in the flat-plane V8 engine was observed. Additionally, was noted that second order forces were not influenced by engine operating conditions. Also, the results revealed that due to use of incorrect counterweights, there was greater unbalance in vertical forces than horizontal forces being most critical on the middle bearing.

Future works should analyze the structural stress through finite element (FE) simulations and the performance should be improved through refinement and optimization of the GT-Power computational model. Besides, correct counterweights must be designed to mitigate the unbalanced forces acting on the engine.

5. REFERENCES

Bopaiah, Karan, and Stephen Samuel. 2020. “Strategy for Optimizing an F1 Car’s Performance Based on FIA Regulations.” *SAE International Journal of Advances and Current Practices in Mobility-V129-99EJ*: 15. https://www.sae.org/content/2020-01-0545/.

Boretti, Albert. 2013. “F1 2014: Turbocharged and Downsized Ice and Kers Boost.” *World Journal of Modelling and Simulation* 9(2): 150–60.

Chiodi, Marco et al. 2011. “Improvement of a High-Performance CNG-Engine Based on an Innovative Virtual Development Process.” *SAE Technical Papers*.

Corvaglia, Giovanni, Matthias Böger, and Vincenzo Bevilacqua. 2019. “Cylinder Individual Cam Timing in a V8 Engine.” *MTZ worldwide* 80(4): 44–49. http://link.springer.com/10.1007/s38313-019-0015-2.

Costa, M. 2020. “Cross-Plane vs Flat-Plane Crankshaft.” *ATA*. https://www.advancedta.com/blog/2019/12/30/cross-plane-vs-flat-plane-crankshaft (June 21, 2021).

Heisler, Heinz. 2002. *Advanced Engine Technology*. 2nd ed. ed. Butterworth-Heinemann.

Heywood, John B. 2018. *Internal Combustion Engines Fundementals*. 2nd ed. McGraw-Hill.

Hiscutt, P., and S. Ishikawa. 2008. “Development of Exhaust Sound Quality on Aston Martin V8 Vantage.” *SAE International Journal of Passenger Cars - Mechanical Systems* 1(1): 2008-01–0895. https://www.sae.org/content/2008-01-0895/.

Hoag, Kevin, and Brian Dondlinger. 2016. *Vehicular Engine Design*. Vienna: Springer Vienna. http://link.springer.com/10.1007/978-3-7091-1859-7.

Khanna, Rishabh et al. 2019. “Design and Development of a Dry Sump Lubrication System for a Formula SAE Race Car.” https://www.sae.org/content/2019-26-0026/.

Luján, José M., Vicente Bermúdez, Carlos Guardiola, and Ali Abbad. 2010. “A Methodology for Combustion Detection in Diesel Engines through In-Cylinder Pressure Derivative Signal.” *Mechanical Systems and Signal Processing* 24(7): 2261–75.

Manning, John. 2012. *Internal Combustion Engine Design*. 1st ed.

McLaren. 2016. “History of the F1 Engine.” *McLaren*. https://www.mclaren.com/racing/car/history-of-the-f1-engine/

(June 22, 2021).
McLuckie, Ian, and Scott Barrett. 2005. "V8 Engine Bearing Dynamics: High Perfomance With Minimum Friction." In *Volume 1: 20th Biennial Conference on Mechanical Vibration and Noise, Parts A, B, and C*, ASMEDC, 799–807. https://asmedigitalcollection.asme.org/IDETC-CIE/proceedings/IDETC-CIE2005/47381/799/316527.
Meechan, Mike. 2006. "Motorsports Industry Knowledge Exchange (MiKE): Oxymoron or Holy Grail (An Imperative for Sustaining Regional, National and Global Competitiveness)." In *SAE Technical Paper*, https://www.sae.org/content/2006-01-3610/.
Osman, Azmi. 2012. "Design Concept and Manufacturing Method of a Lightweight Deep Skirt Cylinder Block." https://www.sae.org/content/2012-01-0406/.
Penzel, M, V Belivacqua, and T Raab. 2017. "Porsche Works Cited: The Engine Architeture of V8 Machines." *Porche Newsroom*. https://newsroom.porsche.com/en/innovation/engineering/porsche-engineering-eight-cylinder-engine-configuration-power-machine-14034.html (June 12, 2021).
STĘPIEŃ, Zbigniew. 2016. "A New Generation of F1 Race Engines – Hybrid Power Units." *Combustion Engines* 167(4): 22–37. http://www.combustion-engines.eu/A-new-generation-of-F1-race-engines-hybrid-power-units,116458,0,2.html.

6. APPENDIX

Table 4 – GT-Power engine model details.

Property	**Value**	**Unit**
Heat Transfer Model	WoschiniGT	
Combustion	SIWiebe	
CA 50% MFB	8	deg ATDCf
CA 90% - 10% MFB	32	deg
Wiebe Exponent	2	
Fraction Fuel Burned	99.80%	
Injector Delivery Rate	30	g/s
Number of Injectors per Cylinder	1	
Relative fuel-air ratio (a.k. Lambda)	0.9	
Throttle Angle	90	deg
Maximum Intake Valve Lift	8.4	mm
Maximum Exhaust Valve Lift		mm
Intake Valve Closure	90	deg BTDCf
Exhaust Valve Closure	70	deg ATDCg
Intake Valve Opening	45	deg BTDCg
Exhaust Valve Opening	115	deg ATDCf
Piston Mass	285	g
Connecting Rod Mass	395	g
Connecting Rod Rotating Mass	297.36	g
Counterweight Mass	1091.302	g
Counterweight Moment of Inertia	1504.762	kg.mm²
Counterweight Mass Center X	0.0017	mm
Counterweight Mass Center Y	-8.2449	mm
Counterweight Mass Center Z	8.8311	mm
Counterweight Material	Steel	
Oil	SAE15W40	
Flywheel Mass	7.4	
Flywheel Moment of Inertia Izz	789821.21	kg.mm²
Flywheel Moment of Inertia Ixx	40101.34	kg.mm²
Flywheel Moment of Inertia Iyy	40103.49	kg.mm²